Supporting Information

Can Cyclopropyl Ring Serve as Energetic Moiety? A Structural and Reactivity Perspective

Sonali Kukreja, Anupama K and Srinivas Dharavath*

Energetic Materials Laboratory, Department of Chemistry, Indian Institute of Technology Kanpur, Kanpur-208016, Uttar Pradesh, India. E-mail: srinivasd@iitk.ac.in

Table of Contents

Experimental Section:

Caution! The compounds in this work are energetic materials that could potentially explode under certain conditions (e.g., impact, friction, or electric discharge). Appropriate safety precautions, such as the use of shields in a fume hood and personal protection equipment (safety glasses, face shields, ear plugs, as well as gloves) should always be taken when handling these materials.

General. All reagents were purchased from AKSci or TCI or Merck in analytical grade and were used as supplied. ^{1}H, and $^{13}C\{^{1}H\}$ spectra were recorded using JEOL DELTA (ECS) 500 (^{1}H, 500 MHz) and $^{13}C\{1H\}$ NMR (126 MHz, $DMSOd_6$) nuclear magnetic resonance spectrometer. Chemical shifts for ^{1}H NMR and $^{13}C\{1H\}$ NMR spectra are given with respect to external $(CH_3)_4Si$ (^{1}H and ^{13}C). [D6] DMSO was used as a locking solvent unless otherwise stated. IR spectra were recorded using Zn-Se pellets with a ECO-ATR spectrometer (Bruker Alpha II). A single crystal of suitable dimensions was used for data collection. Diffraction intensities were collected on a Bruker APEX-II CCD diffractometer, with graphite monochromated Mo Kα (0.71073 Å) radiation at 100(2) K. Using Olex2,[1] the structure was solved with the Olex2.Solve[2] structure solution program using charge flipping and refined with the SHELXL.[3] Density was determined at room temperature by employing Anton Par Ultra5000 gas pycnometer. Mass data was recorded using LC-MS (ESI)-Q-TOF (Agilent 6546) mass spectrometer. The heat of combustion was measured by bomb calorimetry (Parr 6200), under O_2 pressure of 32 MPa. Decomposition temperatures (onset) were recorded using a dry nitrogen gas purge and a heating rate of 5 °C min^{-1} on a thermogravimetric differential scanning calorimeter (TGA-DSC (SDT-650)). Impact and friction sensitivity measurements were made using a standard BAM fall hammer and a BAM friction tester.

Synthesis of 6-dicyclopropyl-5-nitropyrimidine-4,6-diamine (2): 4,6-Dichloro-5-nitropyrimidine (**1**) (2.0 g, 10.31 mmol) was suspended in THF, followed by the sequential addition of triethylamine (2.29 g, 22.68mmol) and cyclopropylamine (1.29 g, 22.68 mmol). The reaction mixture was refluxed for 12 h, after which the solvent was removed under reduced pressure. The resulting residue was treated with water, leading to the formation of a shiny yellow precipitate. The solid was filtered, washed with water, and dried to yield compound **2**. Yield (1.94 g, 8.24 mmol, 80%) ^{1}H NMR (500 MHz, DMSO-d6): δ 9.07 (s, 1H), 9.06 (s, 1 H) 8.17 (s, 1H), 3.13 (m, 2H), 0.82 (m, 4H), 0.74 (m, 4H). $^{13}C\{1H\}$ NMR (126 MHz, DMSOd6) δ 159.93, 158.42, 112.85, 25.36, 7.26. IR (ATR ZnSe): 3313, 1578, 1496, 1350, 1286, 1258,

1160, 1070, 1006, 926, 783, 644 cm^{-1}. HRMS (ESI-QTOF) m/z: $(M+H)^+$ Calcd for $C_{10}H_{13}N_5O_2$: 236.1147; Found: 236.1147. Elemental Analysis Calcd for $C_{10}H_{13}N_5O_2$: C, 51.06; H, 5.57; N, 29.77. Found: C, 51.00; H, 5.49; N, 29.68.

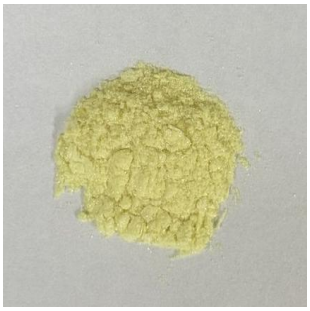

Synthesis of 4,6-bis(cyclopropylamino)-5-nitropyrimidin-2(1H)-one (3): Compound **2** (1 g, 4.25 mmol) was dissolved in trifluoroacetic acid (4 mL) at 50 °C until a homogeneous solution was obtained. A 30% aqueous hydrogen peroxide solution (1 mL) was then added dropwise over a period of 15 minutes under continuous stirring. The reaction mixture was maintained at 50 °C for 12 h, leading to the formation of a clear solution. Upon completion, the solvent was removed under reduced pressure, and the resulting residue was treated with water to precipitate compound **3** as a white solid, which was isolated by filtration and dried. Yield (0.80 g, 3.18 mmol, 75%). ^{1}H NMR (500 MHz, DMSO-d6): δ 9.63 (s, 2H), 2.96 (m, 2H), 0.89 (m, 4H), 0.75 (m, 4H). $^{13}C\{^1H\}$ NMR (126 MHz, DMSO-d6) δ 154.77, 146.33, 106.60, 25.75, 8.69. IR (ATR ZnSe): 3311, 3110, 1660, 1620, 1552, 1499, 1419, 1358, 1298, 1192, 1140, 1016, 825, 770, 664 cm^{-1}. HRMS (ESI-QTOF) m/z: $(M+H)^+$ Calcd for $C_{10}H_{13}N_5O_3$: 252.1097; Found: 252.1092. Elemental Analysis Calcd for $C_{10}H_{13}N_5O_3(0.2\ H_2O)$: C, 47.13; H, 5.30 ; N, 27.48. Found: C, 47.23 ; H, 5.32 ; N, 27.54.

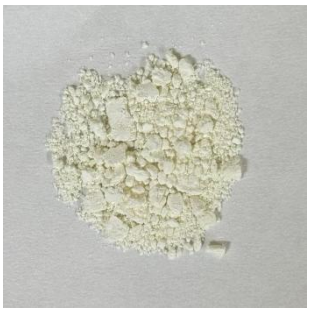

Synthesis of 2,4,6-tricyclopropylpyrimidine-2,4,6-triamine (5): An excess of cyclopropylamine (6 mL) was taken in a round-bottom flask and cooled to 0 °C. 2,4,6-Trichloropyrimidine (**4**) (1 g, 5.45 mmol) was then added dropwise under stirring, and the reaction mixture was maintained at the same temperature for 15 min. Subsequently, the mixture

was allowed to warm to room temperature and then refluxed for 18 h. After completion, the solvent was removed under reduced pressure, and the residue was treated with acetonitrile to afford compound **5** as an off-white precipitate Yield (0.80 g, 3.26 mmol, 60 %). ^{1}H NMR (500 MHz, DMSO-d6): δ 8.20 (s, 1H), 7.40 (s, 2H), 5.64 (s, 1H), 2.54 (t, 3H), 0.71 (t, 6H), 0.45 (t, 6 H). ^{13}C{^{1}H} NMR (126 MHz, DMSO-d6) δ 165.57, 159.05, 158.96, 23.62, 7.05. IR (ATR ZnSe): 3212, 3066, 1575, 1407, 1344, 1263, 1206, 1169, 1090, 1021, 971, 895, 806, 768, 701, 649 cm^{-1}. HRMS (ESI-QTOF) m/z: $(M+H)^+$ Calcd for $C_{13}H_{19}N_5$: 246.1719; Found: 246. 1717.Elemental Analysis Calcd for $C_{13}H_{19}N_5$: C, 63.65; H, 7.81; N, 28.55. Found: C, 63.60; H, 7.76 ; N, 28.45.

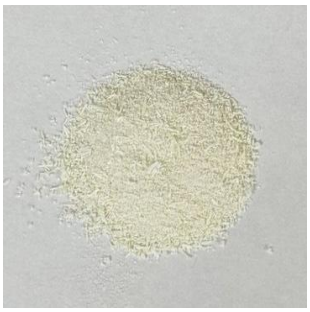

Synthesis of 2,4,6-tricyclopropyl-1,3,5-triazine-2,4,6-triamine (7): 2,4,6-Trichloro-1,3,5-triazine (**6**) (1 g, 5.42 mmol) was suspended in ethanol and cooled to 0 °C. Triethylamine (1.81 g, 17.89 mmol) and cyclopropylamine (1.02 g, 17.89 mmol) were sequentially added dropwise under stirring, and the reaction mixture was maintained at this temperature for 15 min. It was then allowed to warm to room temperature and subsequently refluxed for 12 h. After completion, the solvent was removed under reduced pressure, and the residue was purified by column chromatography (silica gel, hexane/EtOAc, 3:1) to afford compound **7** as a cream-coloured product. Yield (0.60 g, 2.43 mmol, 45%). ^{1}H NMR (500 MHz, DMSO-d6): δ 7.99 (m, 3H), 2.85 (m, 3H), 0.67 (m, 6H), 0.49 (m, 6H). ^{13}C{^{1}H} NMR (126 MHz, DMSO-d6) δ 168.60, 24.05, 6.68. IR (ATR ZnSe): 3232, 3082, 3008, 2933, 1589, 1535, 1398, 1340, 1273, 1213, 1166, 1017, 971, 886, 802, 734, 682 cm^{-1}. HRMS (ESI-QTOF) m/z: $(M+H)^+$ Calcd for $C_{12}H_{18}N_6$: 247.1672; Found: 247.1663. Elemental Analysis Calcd for $C_{12}H_{18}N_6$: C, 58.51; H, 7.37; N, 34.12. Found: C, 58.43; H, 7.32; N, 34.04.

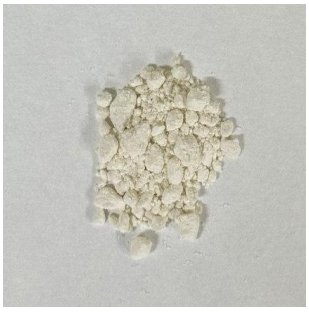

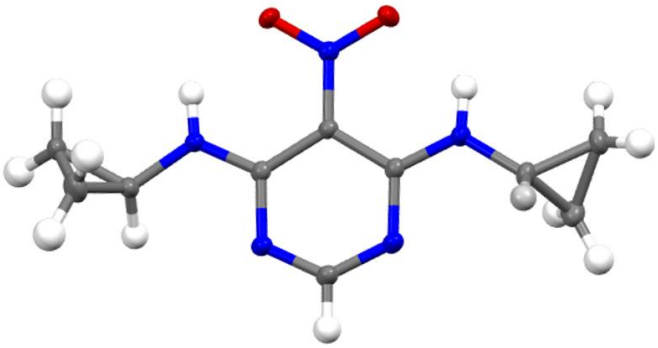

Figure S1: Crystal Structure of **2**.

Table S1. Crystal data and structure refinement for Compound **2.**

Identification code	2540887
Empirical formula	$C_{10}H_{13}N_5O_2$
Formula weight	235.25
Temperature/K	100.0
Crystal system	monoclinic
Space group	P21/n
a/Å	10.1778(4)
b/Å	5.2062(2)
c/Å	21.0514(8)
α/°	90
β/°	97.1250(10)
γ/°	90
Volume/Å3	1106.85(7)
Z	4
ρcalcg/cm3	1.412
μ/mm-1	0.103
F(000)	496.0
Crystal size/mm3	0.14 × 0.13 × 0.1
Radiation	MoKα (λ = 0.71073)
2Θ range for data collection/°	4.692 to 56.668
Index ranges	-13 ≤ h ≤ 13, -6 ≤ k ≤ 6, -28 ≤ l ≤ 28
Reflections collected	16372
Independent reflections	2745 [Rint = 0.0302, Rsigma = 0.0207]
Data/restraints/parameters	2745/0/158
Goodness-of-fit on F2	1.107
Final R indexes [I>=2σ (I)]	R1 = 0.0379, wR2 = 0.1078
Final R indexes [all data]	R1 = 0.0453, wR2 = 0.1239
Largest diff. peak/hole / e Å-3	0.37/-0.29

Figure S2: Crystal Structure of **3**.

Table S2. Crystal data and structure refinement for Compound **3.**

Identification code	2540888
Empirical formula	$C_{10}H_{13}N_5O_3$
Formula weight	251.25
Temperature/K	100.0
Crystal system	triclinic
Space group	P-1
a/Å	5.1034(2)
b/Å	10.0245(5)
c/Å	11.6245(5)
α/°	68.3950(10)
β/°	83.137(2)
γ/°	82.244(2)
Volume/Å3	546.28(4)
Z	2
ρcalcg/cm3	1.527
μ/mm-1	0.117
F(000)	264.0
Crystal size/mm3	0.12 × 0.1 × 0.1
Radiation	MoKα (λ = 0.71073)
2Θ range for data collection/°	3.78 to 73.522
Index ranges	-8 ≤ h ≤ 7, -14 ≤ k ≤ 16, -17 ≤ l ≤ 17
Reflections collected	19102
Independent reflections	4452 [Rint = 0.0459, Rsigma = 0.0449]
Data/restraints/parameters	4452/0/163
Goodness-of-fit on F2	1.054
Final R indexes [I>=2σ (I)]	R1 = 0.0517, wR2 = 0.1384
Final R indexes [all data]	R1 = 0.0777, wR2 = 0.1594
Largest diff. peak/hole / e Å-3	0.58/-0.47

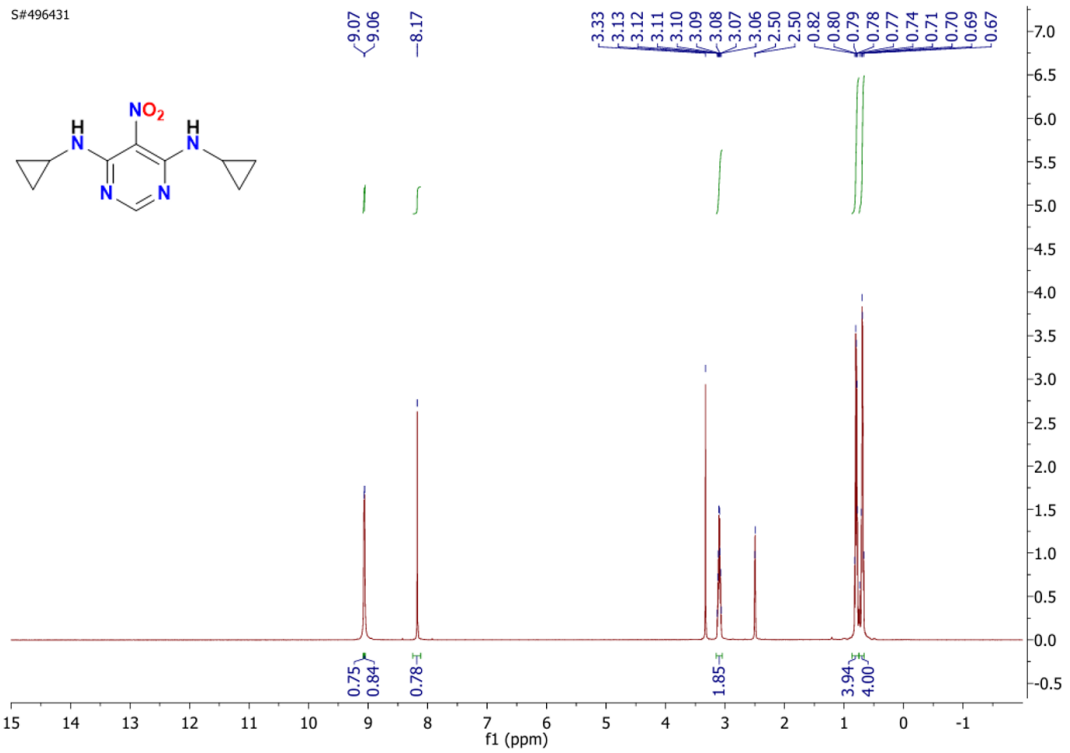

Figure S3: ^{1}H NMR Spectrum of Compound 2 (recorded in DMSO-d6; 500 MHz).

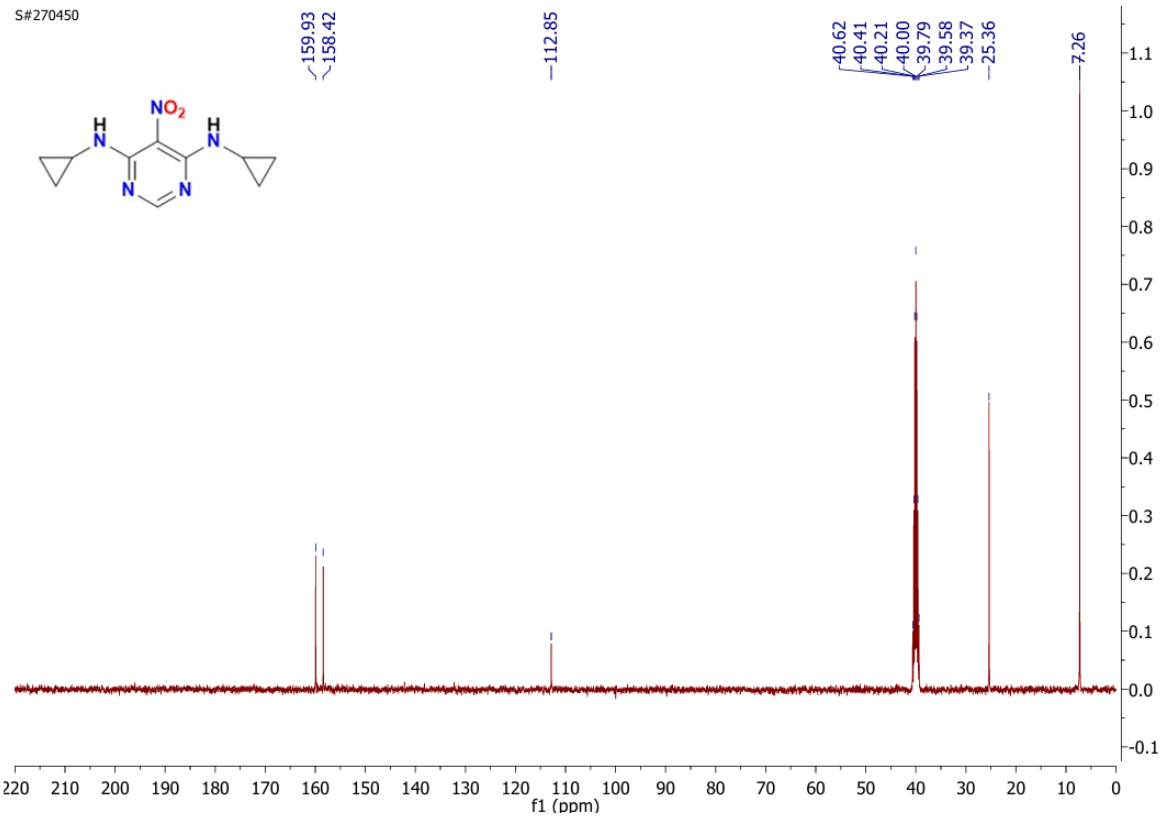

Figure S4: ^{13}C{^{1}H} NMR Spectrum of Compound 2 (recorded in DMSO-d6; 126 MHz).

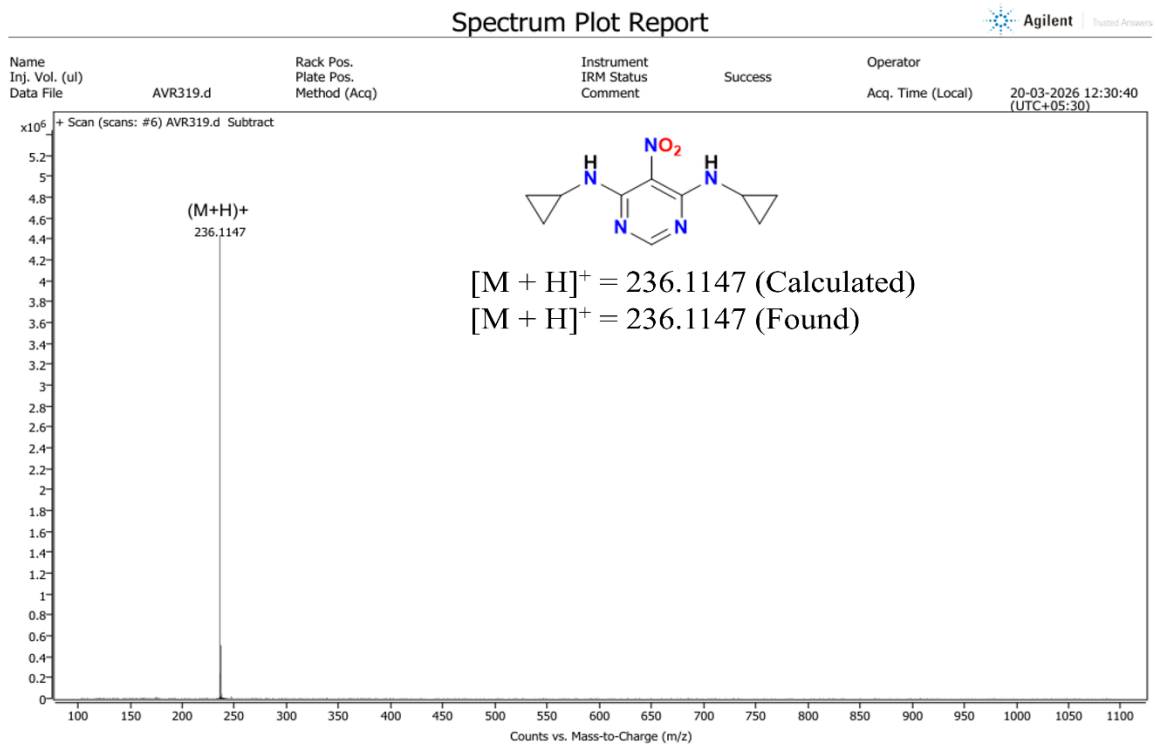

Figure S5: Mass Spectrum of Compound 2

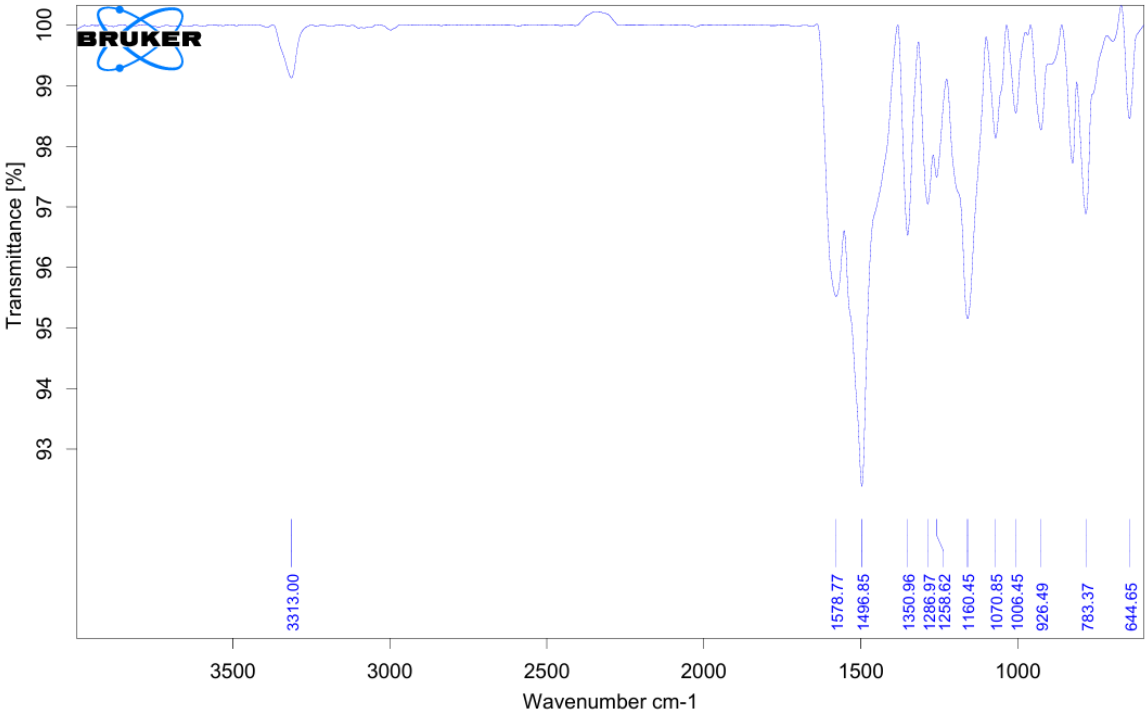

Figure S6: IR Spectrum of Compound 2.

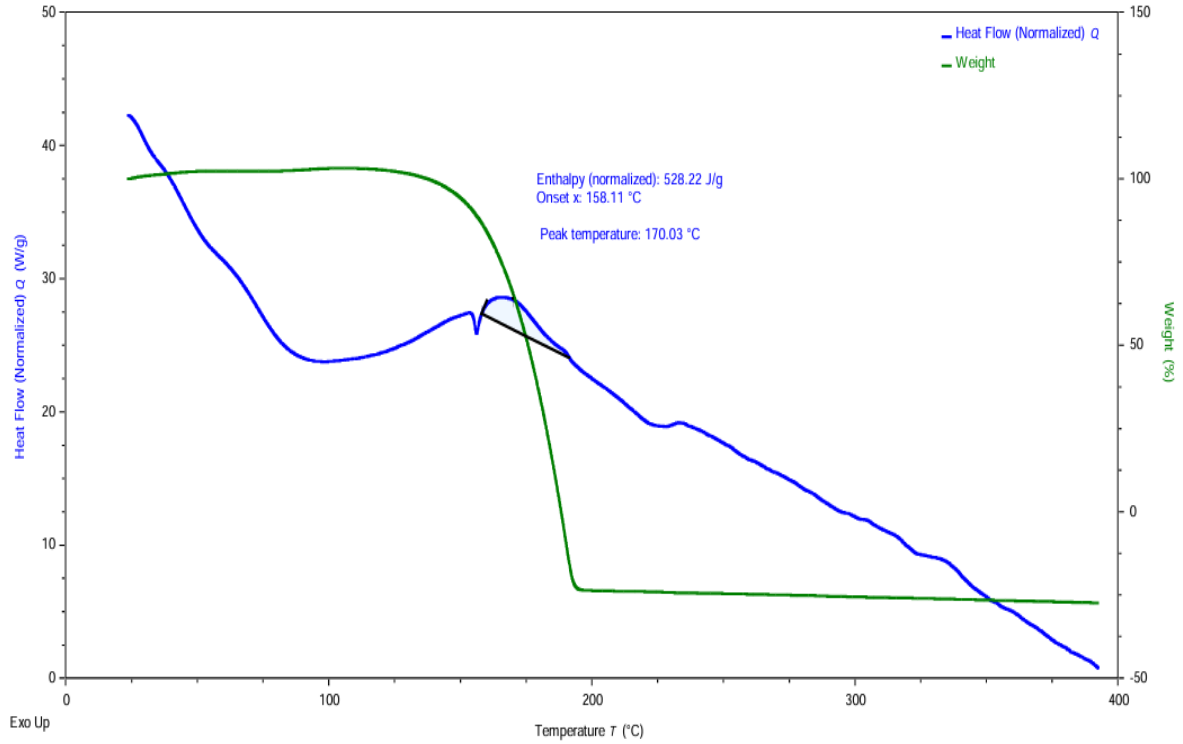

Figure S7: DSC Plot of Compound 2 at Heating rate 5 ^{o}C min^{-1}.

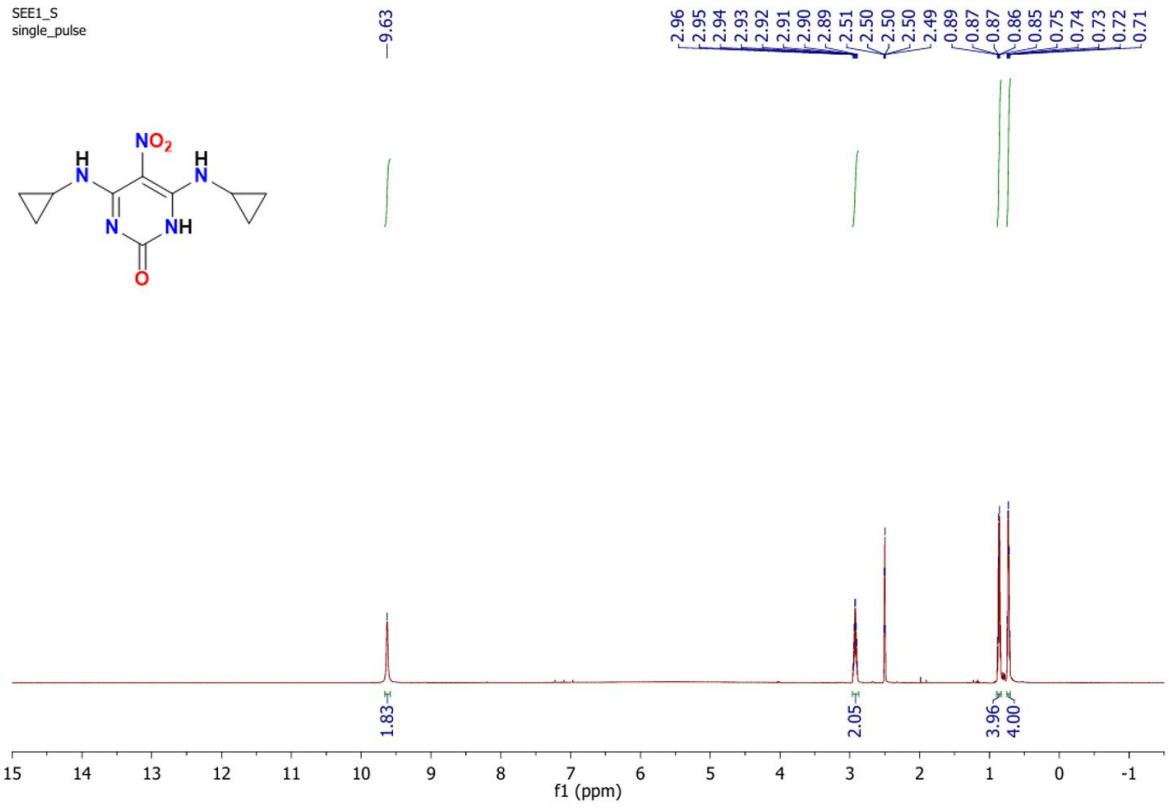

Figure S8: ^{1}H NMR Spectrum of Compound 3 (recorded in DMSO-d6; 500 MHz).

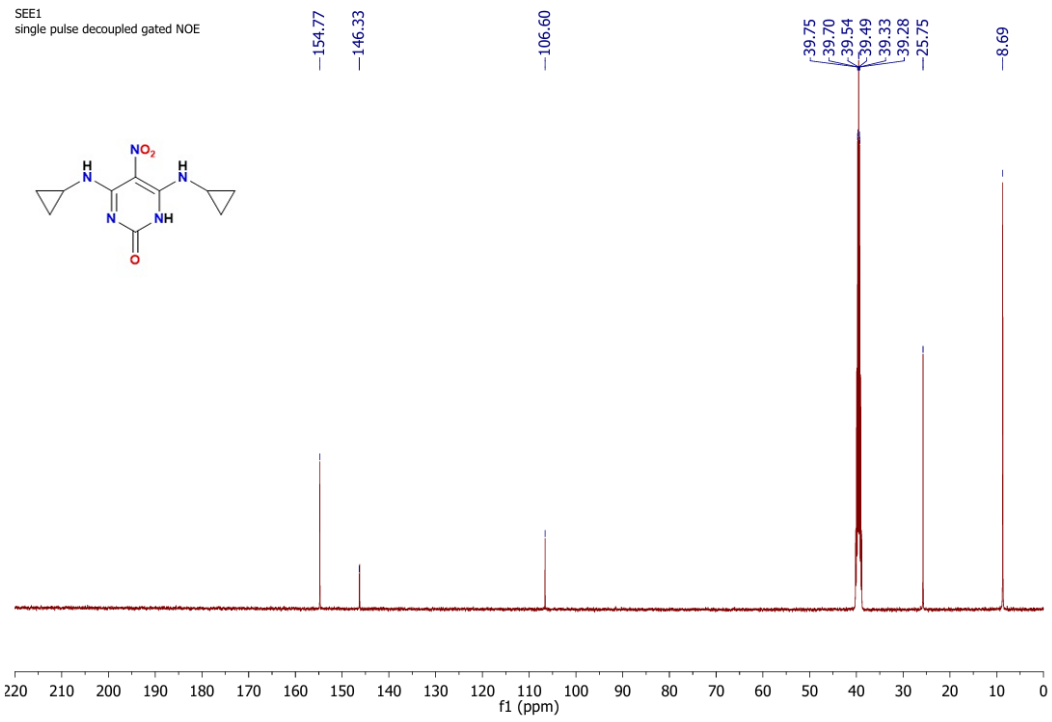

Figure S9: $^{13}C\{^{1}H\}$ NMR Spectrum of Compound 3 (recorded in DMSO-d6; 126 MHz).

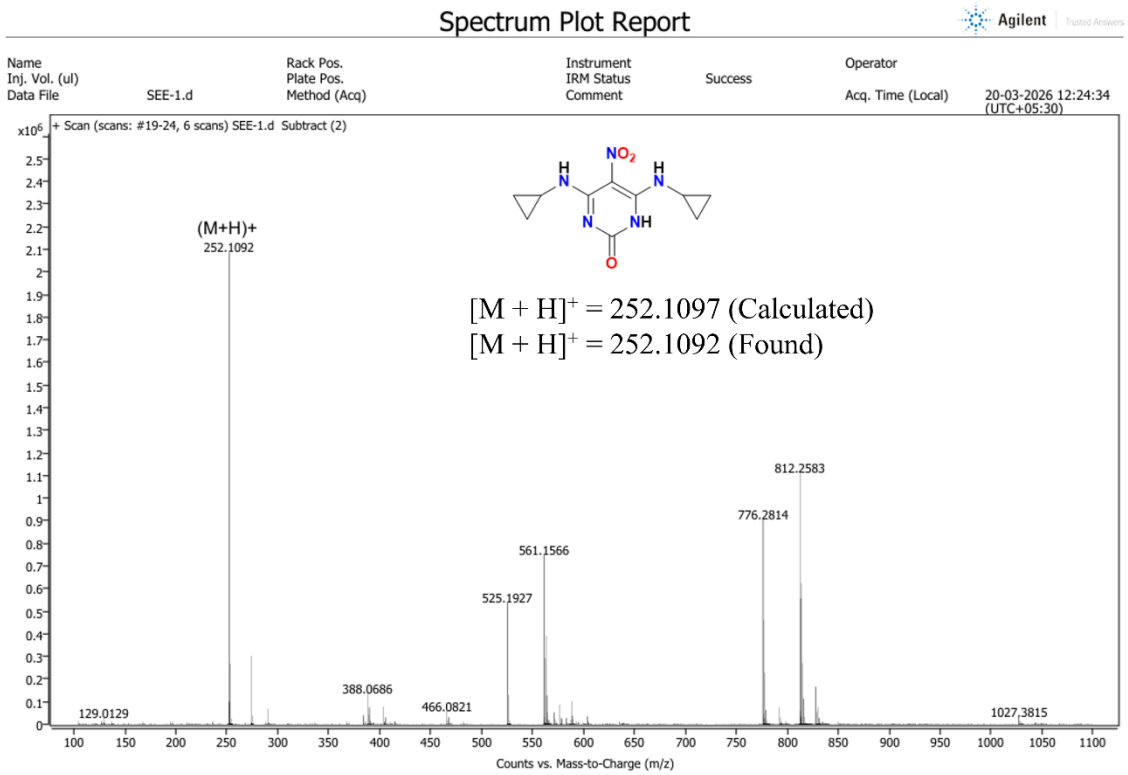

Figure S10: Mass Spectrum of Compound 3.

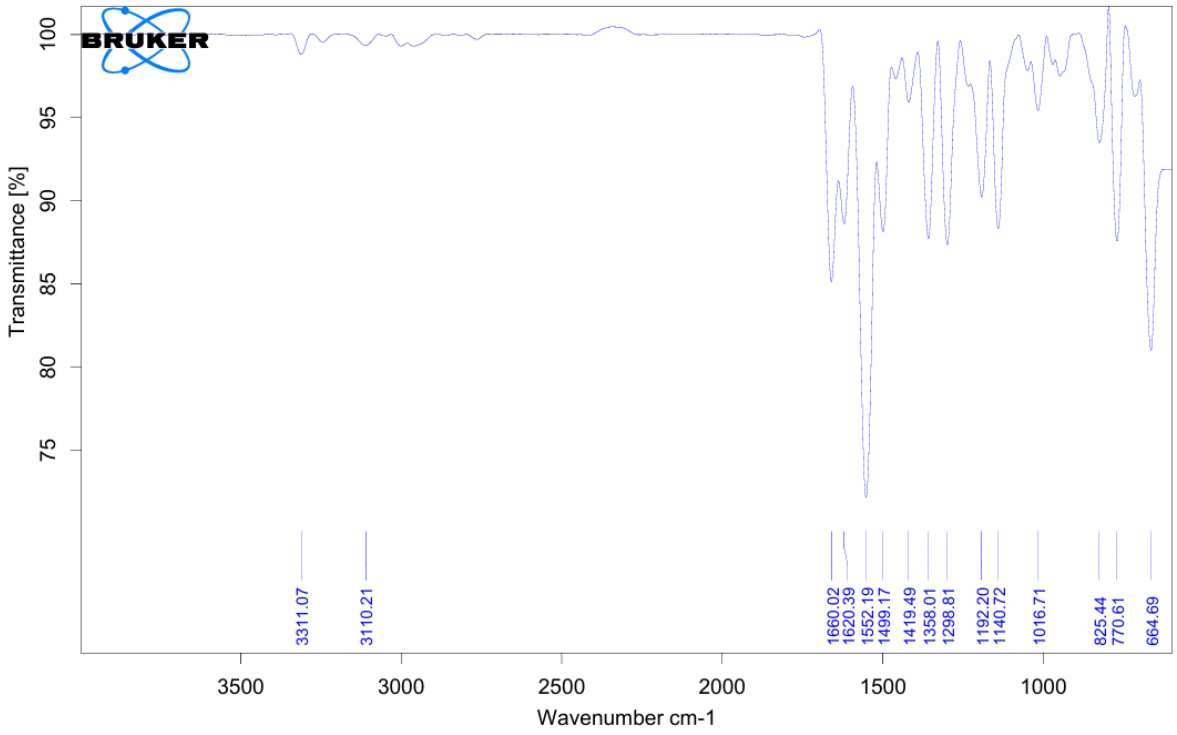

Figure S11: IR Spectrum of Compound 3.

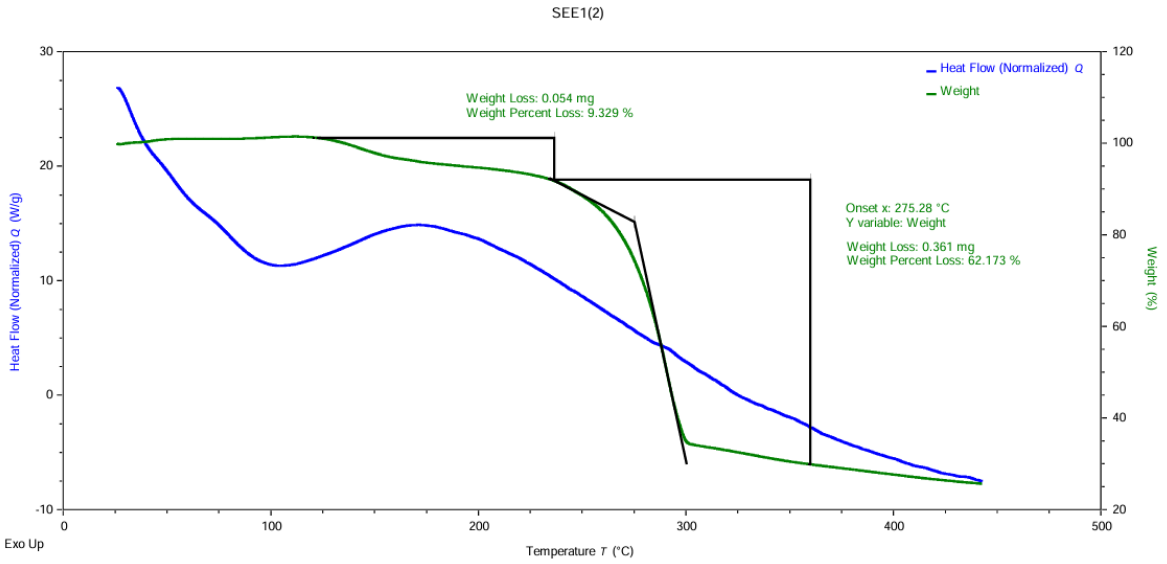

Figure S12: DSC Plot of Compound 3 at Heating rate 5 ^{o}C min^{-1}.

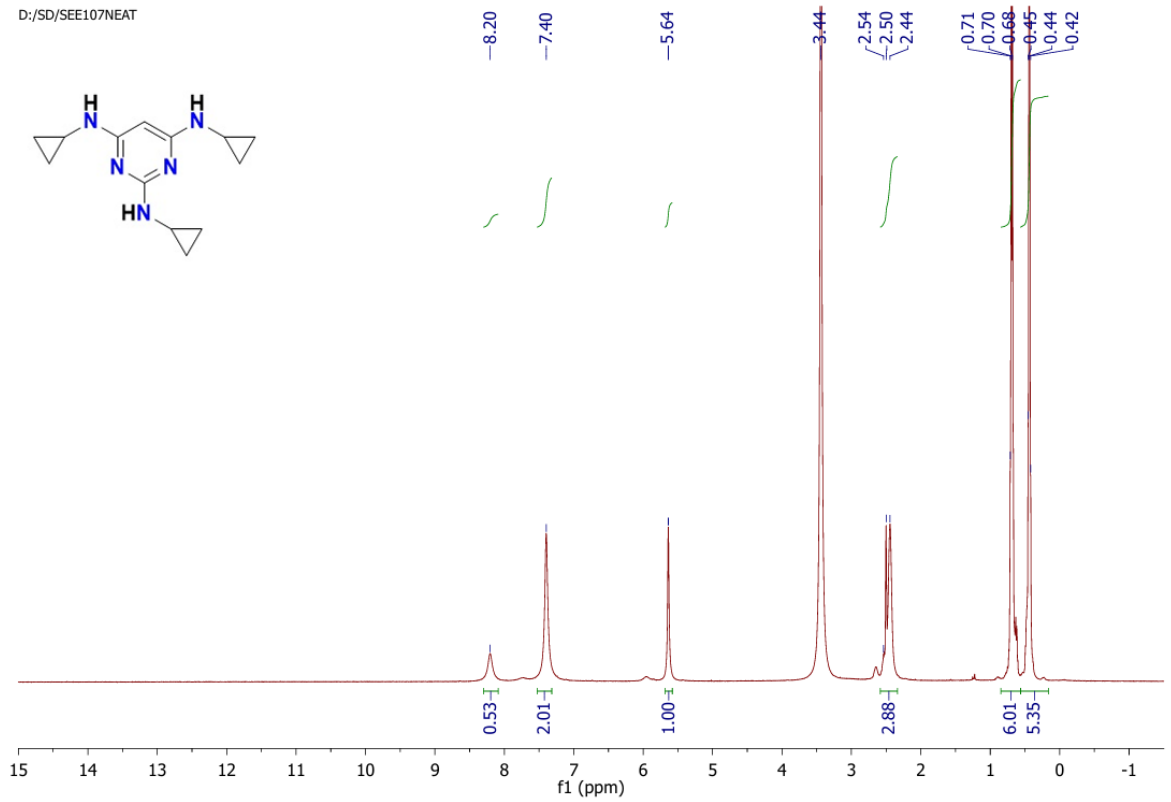

Figure S13: ^{1}H NMR Spectrum of Compound 5 (recorded in DMSO-d6; 500 MHz).

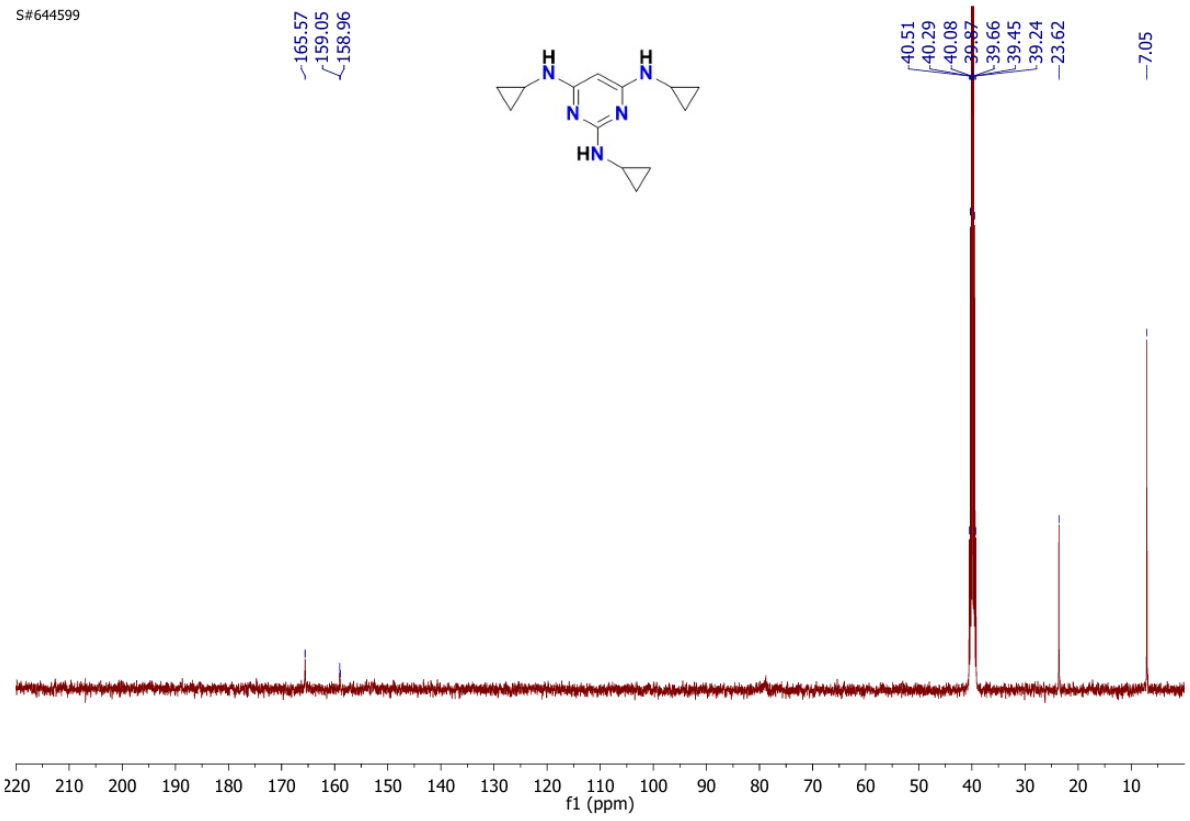

Figure S14: ^{13}C{^{1}H} NMR Spectrum of Compound 5 (recorded in DMSO-d6; 126 MHz).

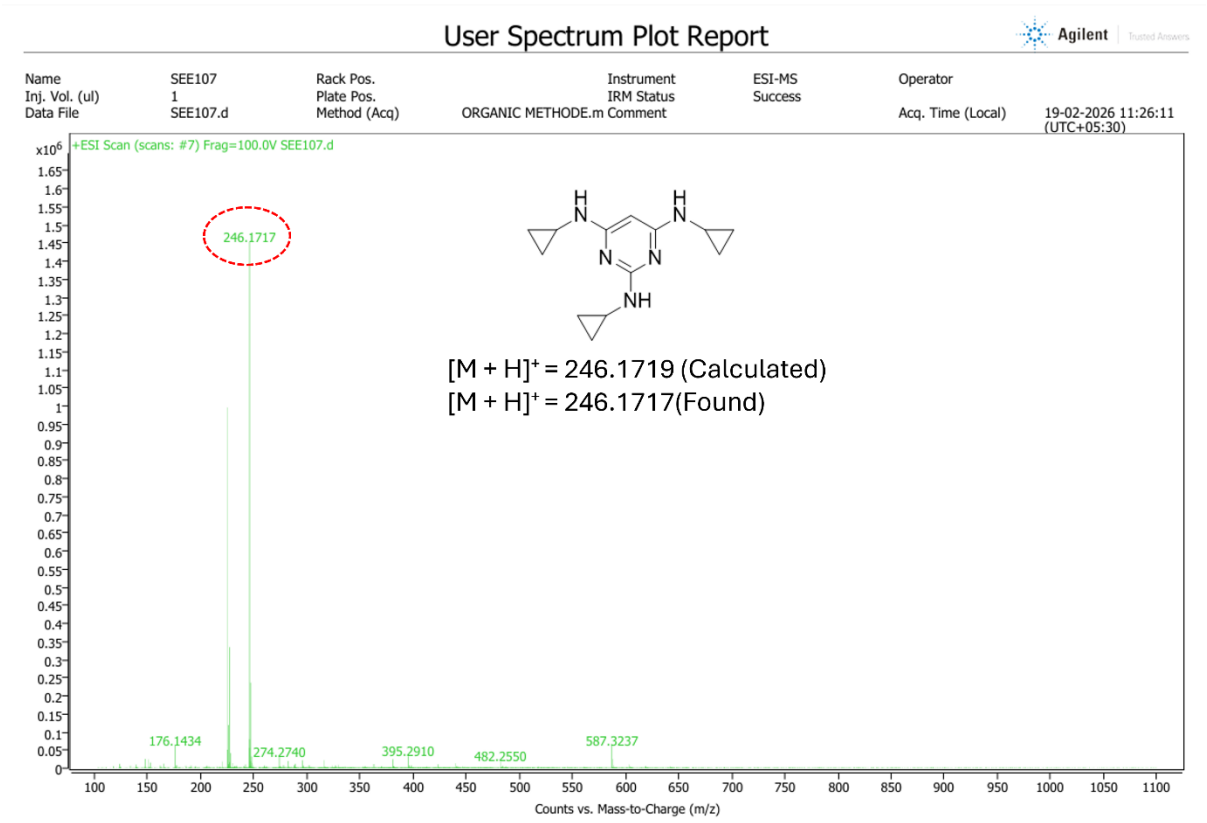

Figure S15: Mass Spectrum of Compound 5.

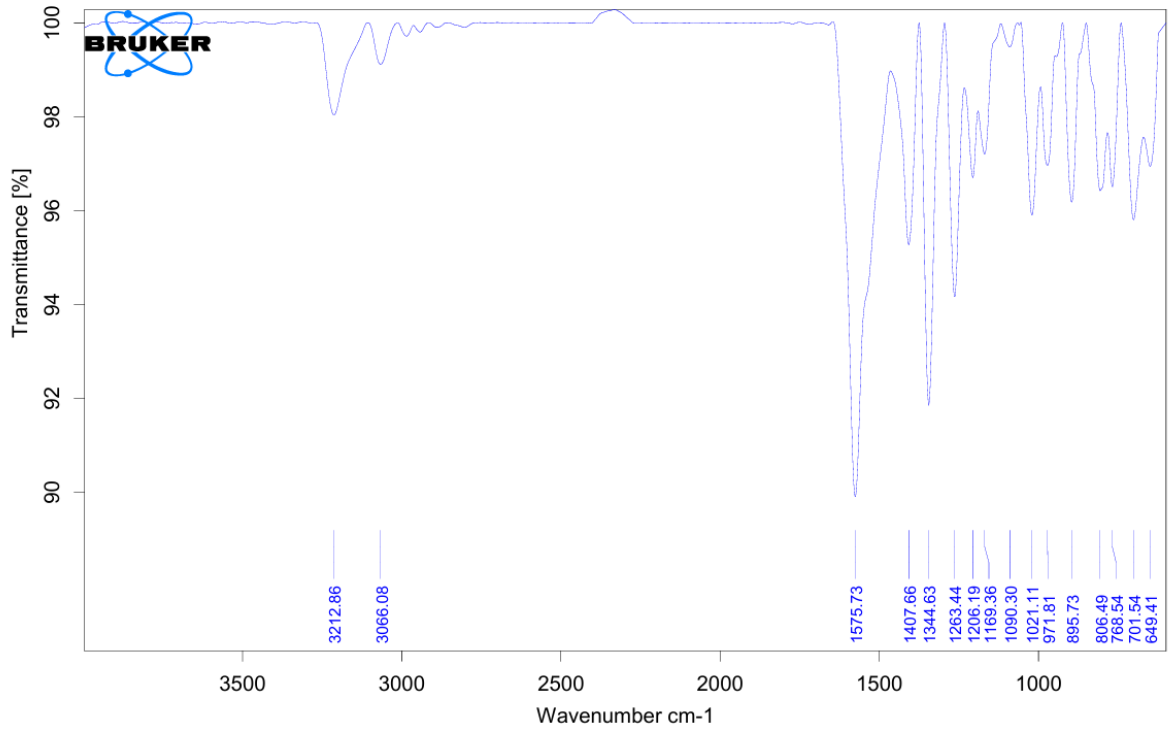

Figure S16: IR Spectrum of Compound 5.

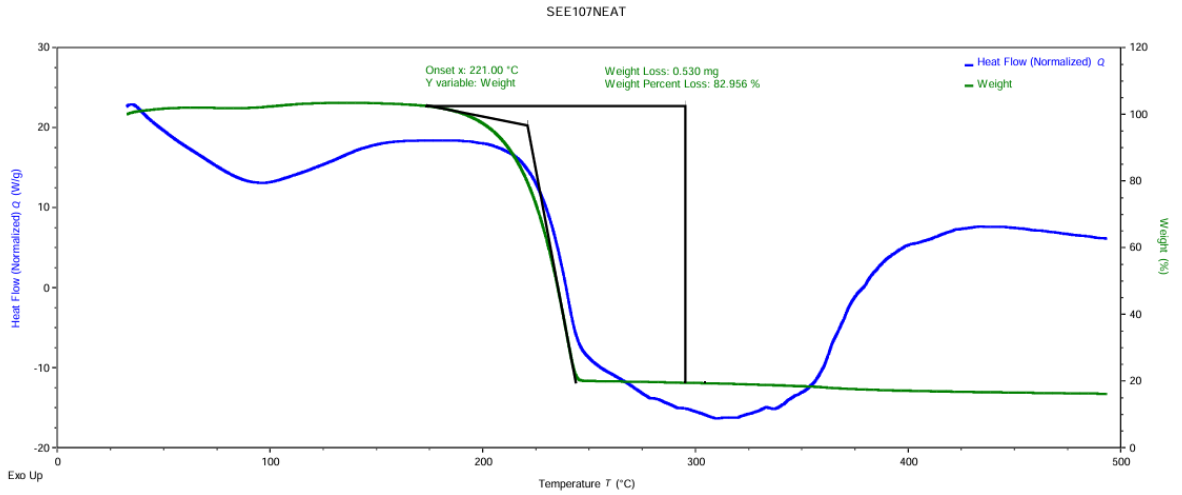

Figure S17: DSC Plot of Compound 5 at Heating rate 5 ^{o}C min^{-1}

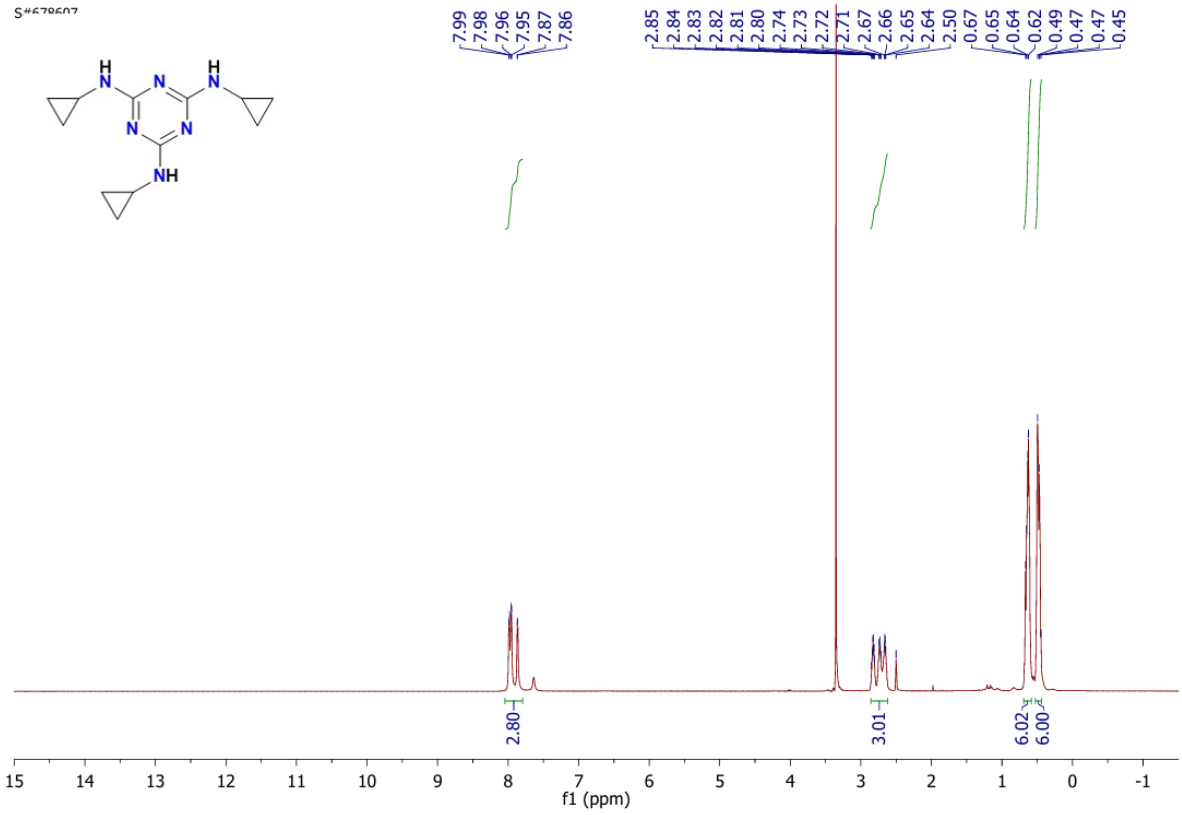

Figure S18: ^{1}H NMR Spectrum of Compound 7 (recorded in DMSO-d6; 500 MHz).

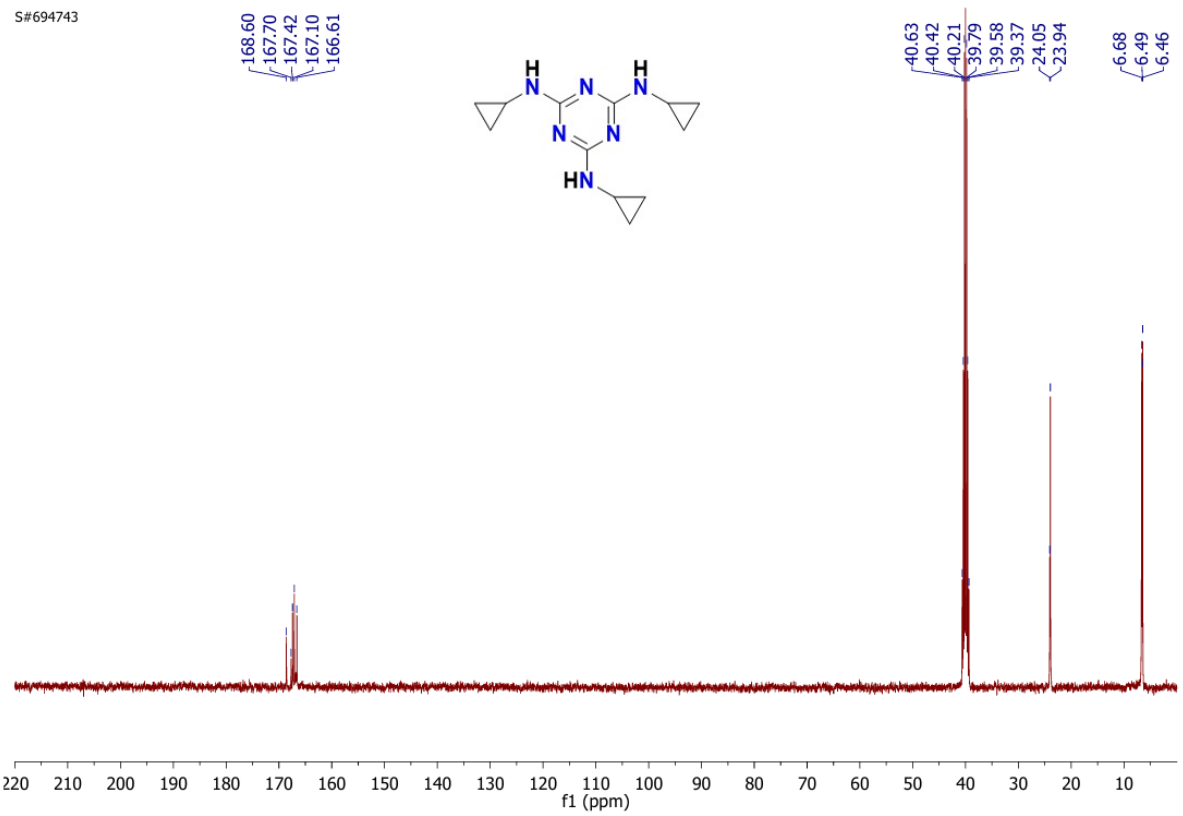

Figure S19: $^{13}C\{^{1}H\}$ NMR Spectrum of Compound 7 (recorded in DMSO-d6; 126 MHz).

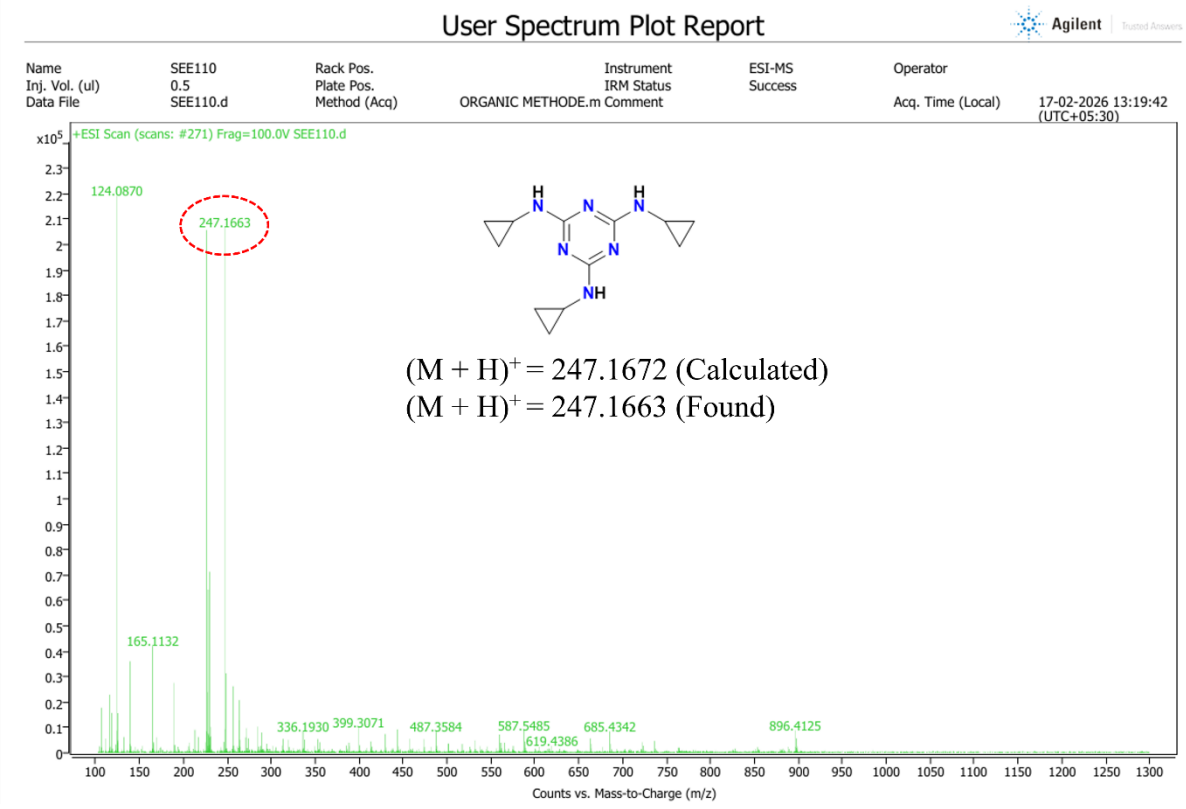

Figure S20: Mass Spectrum of Compound 7.

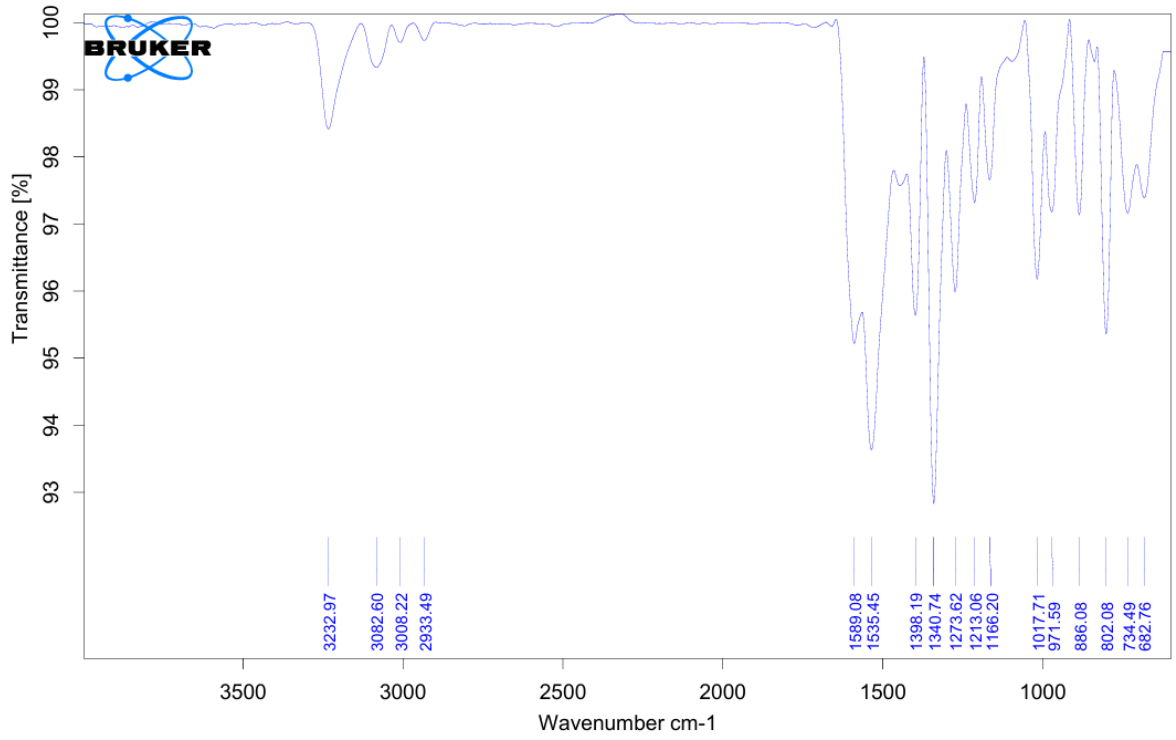

Figure S21: IR Spectrum of Compound 7.

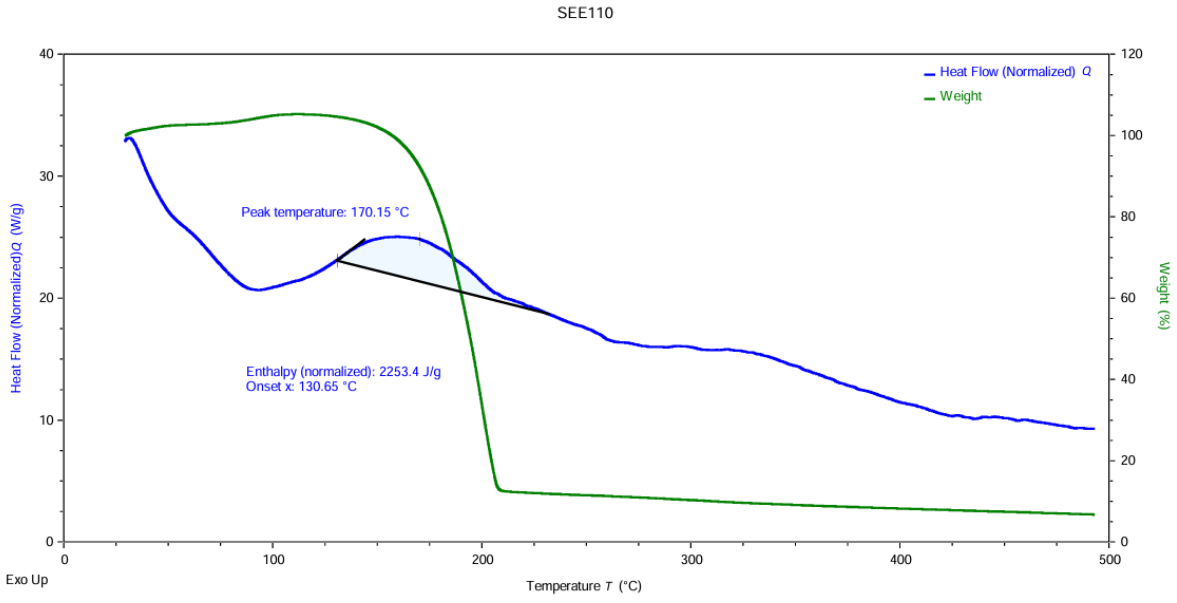

Figure S22: DSC Plot of Compound 7 at Heating rate 5 ^{o}C min^{-1}

Heat of Formation using Bomb Calorimetry

The constant-volume combustion energy of the compounds was measured using a high-precision oxygen bomb calorimeter (Parr 6200). For sample preparation, tablets were formed by mixing each compound with benzoic acid in a 1 : 3 mass ratio (120 mg of compound and

360 mg of benzoic acid). These tablets were sealed in a combustion bomb and ignited in a pure oxygen atmosphere.

The internal energy of combustion (ΔcU) was determined to be −5507.86 kJ mol^{-1} for compound **2** ($C_{10}H_{13}N_5O_2$, MW = 235.24 g mol^{-1}), −5047.22 kJ mol^{-1} for compound **3** ($C_{10}H_{13}N_5O_3$, MW = 251.24 g mol^{-1}), −6453.14 kJ mol^{-1} for compound **5** ($C_{13}H_{19}N_5$, MW = 245.33 g mol^{-1}) and −8453.43 kJ mol^{-1} for compound **7** ($C_{12}H_{18}N_6$, MW = 246.31 g mol^{-1}). The enthalpy of combustion (ΔcH°) was calculated using the relation ΔcH = ΔcU + ΔnRT, where Δn is the change in the number of moles of gaseous products and reactants, R = 8.314 J mol^{-1} K^{-1}, and T = 298.2 K. Based on this, the enthalpies of combustion were found to be -5507.24 kJ mol^{-1} for compound **2** , −5045.36 kJ mol^{-1} for compound **3**, -6458.71 kJ mol^{-1} for compound **5** and -8457.14 kJ mol^{-1} for compound **7**.

The balanced combustion equations for compounds **2**, **3**, **5** and **7** are given below:

$$C_{10}H_{13}N_5O_2 + 12.25\ O_2 \rightarrow 10\ CO_2\ (g) + 6.5\ H_2O\ (l) + 2.5\ N_2\ (g) \quad (1)$$

$$C_{10}H_{13}N_5O_3 + 11.75 O_2 \rightarrow 10\ CO_2\ (g) + 6.5\ H_2O\ (l) + 2.5\ N_2\ (g) \quad (2)$$

$$C_{13}H_{19}N_5 + 17.75\ O_2 \rightarrow 13\ CO_2\ (g) + 9.5\ H_2O\ (l) + 2.5\ N_2\ (g) \quad (3)$$

$$C_{12}H_{18}N_6 + 16.5\ O_2 \rightarrow 12\ CO_2\ (g) + 9\ H_2O\ (l) + 3\ N_2\ (g) \quad (4)$$

The standard enthalpy of formation (ΔfH°) for the newly synthesized compounds **2** , **3**, **5** and **7** are listed in **Table S3**, using Hess's Law, as outlined in eqn (5 - 8) respectively. These calculations were based on the known standard enthalpies of formation for H_2O (l) at −285.83 kJ mol^{-1} and CO_2 (g) at −393.51 kJ mol^{-1}.

Table S3: Experimental enthalpy of formation of compounds 2,3,5 and 7.

S.No	Compound	Experimental Enthalpy of Formation (KJ mol^{-1})
1.	Compound **2**	-285.75
2.	Compound **3**	-747.63
3.	Compound **5**	-1372.30
4.	Compound **7**	1162.55

$$\Delta_f H°[\mathbf{2}, s] = 10\Delta_f H°[CO_2, g] + 6.5\Delta_f H°[H_2O, l] - \Delta cH°[2, s] \quad (5)$$

$$\Delta_f H°[\mathbf{3}, s] = 10\Delta_f H°[CO_2, g] + 6.5\Delta_f H°[H_2O, l] - \Delta cH°[3, s] \quad (6)$$

$$\Delta_f H°[\mathbf{5}, s] = 13\Delta_f H°[CO_2, g] + 9.5\Delta_f H°[H_2O, l] - \Delta cH°[5, s] \quad (7)$$

$$\Delta_f H°[\mathbf{7}, s] = 12\Delta_f H°[CO_2, g] + 9\Delta_f H°[H_2O, l] - \Delta cH°[7, s] \quad (8)$$

Net Heat of Combustion (NHOC), Volumetric heat of combustion (VHOC), Specific Impulse and Density specific Impulse

The energy content of fuels is commonly evaluated using net heat of combustion (NHOC) and volumetric heat of combustion (VHOC). Based on bomb calorimetry measurements, the NHOC and VHOC values of all newly synthesized compounds were determined. Notably, all the newly synthesized compounds **2**, **3**, **5**, and **7** exhibit NHOC values exceeding that of conventional hypergolic hydrazine fuel (19.38 MJ kg^{-1}, see Table **S4**). Similarly, the VHOC values of these compounds also surpass that of hydrazine (19.6 MJ L^{-1}), thus, indicating their potential as solid fuels.

Table S4: Net heat of combustion and Volumetric heat of combustion of the synthesized compounds **2**,**3**, **5**,**7** and hydrazine fuel.

Compound	Net Heat of Combustion (NHOC) (MJ Kg^{-1})	Volumetric Heat of Combustion (VHOC) (MJ L^{-1})
Compound 2	23.26	32.50
Compound 3	19.95	29.93
Compound 5	26.09	35.24
Compound 7	34.27	46.33
N_2H_4[a]	19.38	19.60

a = Ref[4]

EXPLO5 (version 7.01.01) Calculations

Specific Impulse Calculation Results of Fuel 2

Combustion condition: Isobaric combustion (p=const.)

Chamber pressure = 7.000 MPa

Ambient pressure = 0.100 MPa

Expansion conditions: Equilibrium expansion

REACTANT INFORMATION:

1. Fuel **2** = 27.78 %
2. Nitric acid, white fumic (WFNA, HNO_3) = 71.49 %
3. Water (H_2O, liquid) = 0.73 %

C (0.913) H (2.127) N (1.334) O (2.846)

Molecular weight = 77.33

Oxygen balance = -0.9105639 %

Enthalpy of formation = -2801.81 kJ/kg

Internal Energy of formation = -2700.73 kJ/kg

THERMODYNAMIC PROPERTIES OF COMBUSTION PRODUCTS:

PARAMETER	CHAMBER	THROAT	EXIT (Pc/Pe)
Pressure (MPa)	7.000	3.928	0.1000
Pressure ratio (Pc/P)	1.000	1.782	70.000
Temperature (K)	2962.7	2796.0	1744.3
Enthalpy (kJ/kg)	-2801.8	-3291.4	-5698.1
Internal energy (kJ/kg)	-3677.8	-4110.3	-6193.9
Entropy (kJ/K kg)	9.543	9.543	9.543
Qp (kJ/kg)	-4220.7	-4414.2	-5014.4
Mol gas (mol/kg expl.)	35.564	35.230	34.190
Mol tot. (mol/kg expl.)	35.564	35.230	34.190
V (dm^3/kg expl.)	797.1	789.7	766.3
Mass gas (g/kg expl.)	1000.00	1000.00	1000.00
Mass cond. (g/kg expl.)	0.00	0.00	0.00
Mw mean (g)	28.118	28.385	29.248
Density, all prod. (kg/m^3)	7.991	4.796	0.202
Density, gas prod. (kg/m^3)	7.991	4.796	0.202
R (J/kg K)	295.68	292.90	284.25
Cp (J/kgK)	1796.0	1783.6	1644.0

Cv (J/kgK)	1500.3	1490.7	1359.7
Cp/Cv	1.197	1.196	1.209
Sonic velocity (m/s)	1024.0	989.9	770.2
Mach number (m/s)	-	1.000	3.125
Flow velocity (m/s)	-	989.5	2406.8
Mass flux (kg/m^{2}s)	-	4745.54	485.39

PERFORMANCE PARAMETERS:

PARAMETER	THROAT	EXIT (Pc/Pe)
Pressure ratio (Pc/P)	1.782	70.000
Area ratio (Ae/At)	1.000	9.777
Characteristic vel. (m/s)	1475.1	1475.1
Exhaust velocity (m/s)	989.5	2406.8
Thrust coefficient	0.671	1.632

NOTE: Specific impulse at Pc=7.0 MPa, and Pc/Pe=70.00 equals 245.422 s

CONCENTRATION OF COMBUSTION PRODUCTS (mol/kg of explosive) :

PRODUCT	CHAMBER	THROAT	EXIT (Pc/Pe)
C(gr)	0.00000E+00	0.00000E+00	0.00000E+00
CH	1.50663E-11	2.22944E-12	1.28151E-19
CH2	4.30930E-11	7.33460E-12	1.07647E-17
CH2O	1.60986E-06	6.17081E-07	1.75017E-09
CN2	3.39459E-12	5.45829E-13	1.52472E-19
CNO	2.35427E-07	7.23535E-08	1.84603E-12
CO	2.41863E+00	1.96083E+00	4.34293E-01
CO2	9.39046E+00	9.84828E+00	1.13748E+01
H	6.91608E-02	4.78691E-02	5.02248E-04
H2	4.33285E-01	3.57286E-01	1.37176E-01
H2O	1.29742E+01	1.31430E+01	1.36150E+01
H2O2	2.39720E-04	1.23851E-04	2.92904E-08
HCN	6.14849E-07	2.07756E-07	2.85339E-10
HCNO	3.09306E-06	1.23926E-06	3.21157E-09
HN3	8.98477E-12	2.40704E-12	2.94093E-17
HNO	1.15499E-04	5.53433E-05	1.10482E-08
HO2	2.42171E-03	1.32100E-03	9.69882E-08
N	2.19045E-05	9.07711E-06	2.19432E-10
N2	8.49220E+00	8.53035E+00	8.62464E+00
NH	4.98166E-06	1.81942E-06	6.49991E-11
NH3	1.39336E-05	6.69908E-06	1.72094E-07

NO	2.64897E-01	1.88880E-01	4.42420E-04
NO2	3.33514E-04	1.81775E-04	7.41557E-09
O	5.76626E-02	3.64280E-02	7.18971E-06
O2	8.40044E-01	6.58184E-01	3.83944E-04
OH	6.20255E-01	4.57519E-01	2.66746E-03

Specific Impulse for fuel 5: 227.9 s

The calculated specific impulses for compounds **2** and **5** are 245.4 s and 227.9 s, respectively. In comparison, the Hydrazine-based compound (**iii**) exhibits a specific impulse of 268.3 s. It is evident that Compounds **2** and **5** demonstrate only a moderate reduction in performance, indicating that they retain competitive propulsive characteristics and represent viable alternatives to conventional hydrazine-based systems.

Density Specific Impulse Calculations

Density of Compound **2** = 1.39 g cm^{-3}

Density of Compound **5** = 1.34 g cm^{-3}

Density of White fuming nitric acid = 1.51 g cm^{-3}

Oxidizer to Fuel ratio for fuel **2** = 2.6

Density of fuel **2** propellant = 1 / {(0.28 / 1.39) + (0.72 / 1.51)} = 1.47 g cm^{-3}

ρIsp of fuel **2** propellant = 1.47 x 245.4 = 361 s g cm^{-3}

Oxidizer to Fuel ratio for fuel **5** = 3.6

Density of fuel **5** propellant = 1 / {(0.22 / 1.34) + (0.78 / 1.51)} = 1.47 g cm^{-3}

ρIsp of fuel **5** propellant = 1.47 x 227.9 = 335 s g cm^{-3}

Hirshfeld Surface and 2D-fingerprint plots analysis: Hirshfeld surface analysis, two-dimensional fingerprint plots, and quantitative evaluation of close-contact contributions were performed using CrystalExplorer software[5] to elucidate the relationship between the molecular structures of compound **2** and **3** and their physicochemical properties. The Hirshfeld surfaces of both compounds reveal nearly planar molecular geometries. Prominent red spots are primarily localized on the lateral faces of the molecular plates rather than on the frontal surfaces, indicating that intermolecular interactions are predominantly governed by peripheral atoms (H, O, and N) surrounding the molecular frameworks (**Figures S23a, b and d, e**).

Figures S23c and **S23f** depict the relative percentage contributions of various intermolecular contacts in compound **2** and **3**, respectively. Among these, O···H interactions contribute 17% in compound **2** and 26% in compound **3** of the total weak contacts, while N···H interactions account for 12% and 9% in compound **2** and **3**, respectively. These contacts represent the principal hydrogen-bonding interactions and play a key role in enhancing molecular stability. H···H interactions are the most abundant in both compounds, contributing 52% in compound **2** and 45% in compound **3** of the total weak interactions, and significantly promote lattice stabilization. C···H interactions also make a notable contribution, accounting for 9% and 7% of the total interactions in compound **2** and **3**, respectively. Additional contacts, including O···N and O···C interactions, each contribute approximately 3% in compound **2**, while O···C interactions account for 6% in compound **3**. The presence of O···C contacts suggest face-to-face π–π stacking interactions, which further reinforce the structural integrity of the crystal lattice. Overall, the cumulative dominance of stabilizing intermolecular interactions rationalizes the observed stability and reduced sensitivity of both compounds **2** and **3**.

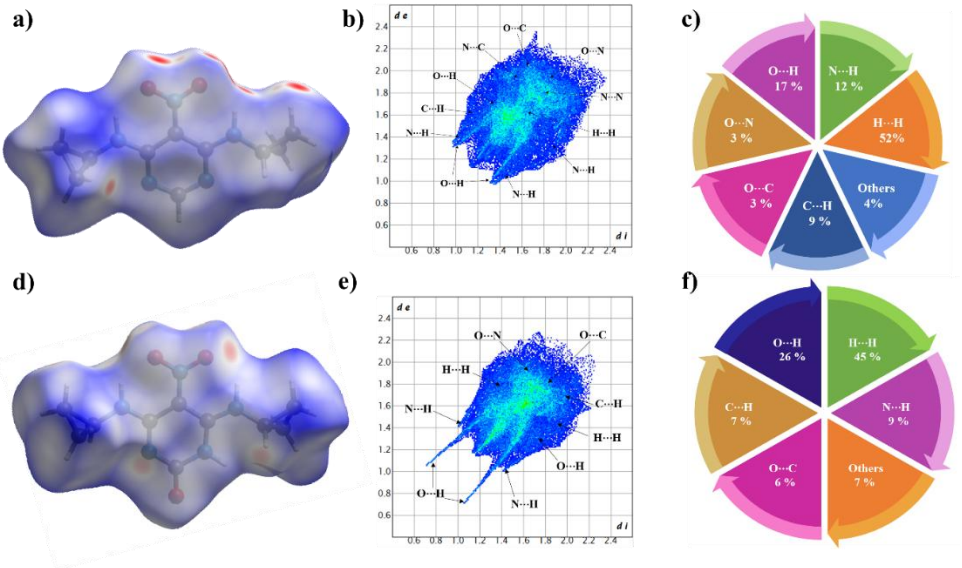

Figure S23: (a, d) Hirshfeld surface of **2** and **3** respectively. (b, e) 2D fingerprint plots in the crystal stacking for **2** and **3** respectively. (c, f) showing % contribution of individual atomic contacts to the Hirshfeld surface of **2** and **3** respectively.

References:

1) O. V. Dolomanov, L. J. Bourhis, R. J. Gildea, J. A. K. Howard and H. Puschmann *J. Appl. Crystallogr.* **2009**, *42*, 339– 341.

2) L. J. Bourhis, O.V. Dolomanov, R. J. Gildea, J. A. K. Howard and H. Puschmann *Acta Crystallogr.* **2015**, *A71*, 59– 75.
3) G. M. Sheldrick, *Acta Crystallogr.* **2015**, *C71*, 3– 8.
4) Y. C. Zhang, J. Nie, J. Cao, Y. Liu, Y. Chen, G. Nie, L. Pan, X. Zhang and J. J. Zou, *Combust. Flame*, 2020, **222**, 252–258.
5) Spackman, P. R.; Turner, M. J.; McKinnon, J. J.; Wolff, S. K.; Grimwood, D. J.; Jayatilaka, D.; Spackman, M. A. CrystalExplorer: A Program for Hirshfeld Surface Analysis, Visualization and Quantitative Analysis of Molecular Crystals. *J. Appl. Crystallogr.* **2021**, *54*, 1006– 1011.